IOP PUBLISHING PHYSICS IN MEDICINE AND BIOLOGY

Phys. Med. Biol. **56** (2011) 3857–3872 doi:10.1088/0031-9155/56/13/008

TIPS bilateral noise reduction in 4D CT perfusion scans produces high-quality cerebral blood flow maps

Adriënne M Mendrik[1,2], Evert-jan Vonken[3], Bram van Ginneken[1,4], Hugo W de Jong[3], Alan Riordan[3], Tom van Seeters[3], Ewoud J Smit[3], Max A Viergever[1] and Mathias Prokop[3,4]

[1] Image Sciences Institute, University Medical Center Utrecht, Heidelberglaan 100, 3584 CX Utrecht, The Netherlands
[2] Biomedical Imaging Group Rotterdam, Erasmus Medical Center, Dr Molewaterplein 50/60, 3015 GE Rotterdam, The Netherlands
[3] Radiology Department, University Medical Center Utrecht, Heidelberglaan 100, 3584 CX Utrecht, The Netherlands
[4] Radboud University Nijmegen Medical Centre, Geert Grooteplein-Zuid 10, 6525 GA Nijmegen, The Netherlands

E-mail: a.m.mendrik@gmail.com

Received 7 November 2010, in final form 9 March 2011
Published 8 June 2011
Online at stacks.iop.org/PMB/56/3857

Abstract

Cerebral computed tomography perfusion (CTP) scans are acquired to detect areas of abnormal perfusion in patients with cerebrovascular diseases. These 4D CTP scans consist of multiple sequential 3D CT scans over time. Therefore, to reduce radiation exposure to the patient, the amount of x-ray radiation that can be used per sequential scan is limited, which results in a high level of noise. To detect areas of abnormal perfusion, perfusion parameters are derived from the CTP data, such as the cerebral blood flow (CBF). Algorithms to determine perfusion parameters, especially singular value decomposition, are very sensitive to noise. Therefore, noise reduction is an important preprocessing step for CTP analysis. In this paper, we propose a time–intensity profile similarity (TIPS) bilateral filter to reduce noise in 4D CTP scans, while preserving the time–intensity profiles (fourth dimension) that are essential for determining the perfusion parameters. The proposed TIPS bilateral filter is compared to standard Gaussian filtering, and 4D and 3D (applied separately to each sequential scan) bilateral filtering on both phantom and patient data. Results on the phantom data show that the TIPS bilateral filter is best able to approach the ground truth (noise-free phantom), compared to the other filtering methods (lowest root mean square error). An observer study is performed using CBF maps derived from fifteen CTP scans of acute stroke patients filtered with standard Gaussian, 3D, 4D and TIPS bilateral filtering. These CBF maps were blindly presented to two observers that indicated which map they preferred for (1) gray/white matter differentiation, (2) detectability of infarcted area and (3) overall image quality. Based on these results, the TIPS bilateral filter ranked

best and its CBF maps were scored to have the best overall image quality in 100% of the cases by both observers. Furthermore, quantitative CBF and cerebral blood volume values in both the phantom and the patient data showed that the TIPS bilateral filter resulted in realistic mean values with a smaller standard deviation than the other evaluated filters and higher contrast-to-noise ratios. Therefore, applying the proposed TIPS bilateral filtering method to 4D CTP data produces higher quality CBF maps than applying the standard Gaussian, 3D bilateral or 4D bilateral filter. Furthermore, the TIPS bilateral filter is computationally faster than both the 3D and 4D bilateral filters.

(Some figures in this article are in colour only in the electronic version)

1. Introduction

Since x-ray radiation increases the risk of inducing cancer (de González and Darby 2004), x-ray computed tomography (CT) scanning is limited by a trade-off between image quality and the amount of radiation exposure to the patient. In general, the radiation dose should be kept as low as reasonably achievable (ALARA) (Prasad *et al* 2004). This is especially important for 4D CT perfusion (CTP) scans (Diekmann *et al* 2010), which consist of multiple sequential 3D CT scans over time after injection of contrast material. The amount of radiation dose that can be used per sequential scan is therefore limited, which results in a high level of noise.

Cerebral CTP scans are acquired to detect areas of abnormal perfusion in patients with cerebrovascular diseases, such as acute stroke (Mayer *et al* 2000, Wintermark 2005, Wintermark *et al* 2009), subarachnoid hemorrhage (Nabavi *et al* 2001) or carotid occlusive disease (Jain *et al* 2004). Detection of these areas is done on perfusion parameter maps of the cerebral tissue showing the cerebral blood volume (CBV), mean transit time (MTT) and cerebral blood flow (CBF) (Hoeffner *et al* 2004). Various algorithms were proposed to determine these perfusion parameters (Konstas *et al* 2009, Ostergaard *et al* 1996b, Wittsack *et al* 2008). Deconvolution-based algorithms are preferred above nondeconvolution-based algorithms, such as the maximum slope method, that generally rely on simplified assumptions regarding the underlying vascular architecture (Konstas *et al* 2009). Of the deconvolution-based algorithms, the model-dependent approaches are more stable, but may lead to large systematic errors in comparing regions with different residue function (Ostergaard *et al* 1996b). Therefore model-independent approaches, in particular singular value decomposition (SVD), are preferred (Ostergaard *et al* 1996b). These approaches are, however, very sensitive to noise because deconvolution of discrete data points leads to oscillations, which strongly depend on the noise level within the processed time curves (Wittsack *et al* 2008). To obtain more robust results, a global noise threshold is used for standard SVD and block-circulant SVD uses an oscillation index. However, even when the oscillation index is used, the quality of the CBF maps decreases drastically with increasing noise level (Wittsack *et al* 2008). Therefore, noise reduction is an important preprocessing step for CTP analysis.

In 4D perfusion data, different tissue types are characterized by differences in the time-intensity profiles (fourth dimension). For instance, healthy tissue has a different time-intensity profile, contrast uptake and wash out than an area at risk of infarction, and the time-intensity profiles of white matter are different from those of gray matter. The main goal of noise

reduction in perfusion data is therefore to reduce noise while preserving the time-intensity profiles that are essential for determining the perfusion parameters.

Kosior *et al* (2007) investigated the effect of 4D Gaussian smoothing and 4D bilateral filtering on CBF maps of magnetic resonance (MR) perfusion scans. Their conclusion was that 4D bilateral filtering was more suited for filtering the MR perfusion data than 4D Gaussian smoothing. Gaussian smoothing could produce larger CBF errors than no filtering, and edges were better preserved by using the 4D bilateral filter. The 4D bilateral filter used by Kosior *et al* (2007) averages similar intensity values in the spatial (three dimensions) and temporal domains. This is beneficial in areas with no contrast enhancement such as the cerebrospinal fluid. In these areas intensity values in the temporal domain can be assumed equal to values in the spatial domain, except for noise. However within areas with contrast enhancement such as the gray and white matter, averaging over different time points can change the contrast enhancement profiles that are important for determining the cerebral tissue perfusion parameters.

In this paper, a bilateral filtering method is proposed that uses the time-intensity profile similarity (TIPS) to reduce noise in the spatial domain. The novelty of the proposed method is twofold. Firstly, time-intensity profiles are preserved while noise is reduced. Secondly, the TIPS bilateral filter is computationally much faster than the 4D bilateral filter. The reason for this is that a 3D kernel instead of a 4D kernel is used, of which the weights are determined once for each spatial position and applied to that same spatial position in all sequential scans. The proposed TIPS bilateral filter is compared to standard Gaussian smoothing, and 4D and 3D (applied to each sequential scan) bilateral filtering on both phantom and real patient CTP data. Following the paper by Kosior *et al* (2007), the main focus of the evaluation is on CBF maps. CBF is defined as the total volume of flowing blood in a given volume in the brain in ml/100 g/min (Konstas *et al* 2009); therefore, it represents a combination of the CBV and the MTT. In acute stroke imaging, infarct core (irreversibly infarcted tissue) is typically defined as the CBV lesion volume and penumbra (severely ischemic but potentially salvageable tissue) as the MTT or CBF lesion volume (Konstas *et al* 2009). However, Kudo *et al* (2010) showed that abnormal CBF areas of delay-insensitive algorithms, such as the block-circulant SVD algorithm used for the evaluation in this paper, correspond well to the final infarct size. An advantage of CT perfusion as opposed to MR perfusion is the linear relationship between contrast concentration and attenuation in CT, which facilitates quantitative (versus relative) measurement of CBF and CBV (Konstas *et al* 2009). Therefore quantitative values for CBF and CBV are given for both the phantom and patient data.

2. Method

Bilateral filtering as introduced by Tomasi and Manduchi (1998) for filtering noise from 2D images uses a combination of domain and range filtering. Each pixel value in the image is replaced with a weighted average of similar and nearby pixel values. The Gaussian closeness function $c(\xi, \mathbf{x})$ is defined as (Tomasi and Manduchi 1998)

$$c(\xi, \mathbf{x}) = \exp\left(-\frac{1}{2}\left(\frac{d(\xi, \mathbf{x})}{\sigma_d}\right)^2\right), \tag{1}$$

where $d(\xi, \mathbf{x})$ is the Euclidean distance between a pixel $\mathbf{x}$ and its neighbor ξ, and the standard deviation (σ_d) determines which distance is considered to be close. The pixel similarity function $s(\xi, \mathbf{x})$ is defined as (Tomasi and Manduchi 1998)

$$s(\xi, \mathbf{x}) = \exp\left(-\frac{1}{2}\left(\frac{\delta(\mathbf{f}(\xi), \mathbf{f}(\mathbf{x}))}{\sigma_r}\right)^2\right), \tag{2}$$

where $\delta(\mathbf{f}(\xi), \mathbf{f}(\mathbf{x}))$ is the absolute intensity difference between $\mathbf{x}$ and ξ. Intensities are considered to be similar when their absolute difference is below the standard deviation (σ_r) of the Gaussian function.

Kosior *et al* (2007) used a straightforward extension of this filter to four dimensions. The 2D kernel used by Tomasi and Manduchi (1998) was replaced by a 4D kernel within which the Euclidean distance and absolute intensity difference were determined. However, the fourth dimension (temporal) is of a different type than the first three dimensions (spatial). In 4D perfusion scans, the fourth dimension provides a measure of voxel similarity. For each voxel within the 3D spatial domain, a time-intensity profile (fourth dimension) is available, which can be used to distinguish between different types of tissues in the perfusion scan.

Therefore, we propose to use a time–intensity profile similarity (TIPS) function instead of the conventional absolute intensity difference similarity function for filtering 4D CTP scans. A 3D weighted averaging kernel is used, in which the weights are based on the 3D Euclidean distance and the similarity of the fourth dimension. The TIPS function ($p(\xi, \mathbf{x})$) is defined as

$$p(\xi, \mathbf{x}) = \exp\left(-\frac{1}{2}\left(\frac{\zeta(\xi, \mathbf{x})}{\sigma_\zeta}\right)^2\right), \tag{3}$$

where $\zeta(\xi, \mathbf{x})$ is the sum of squared differences (SSD) measure between the time-intensity profile at voxel $\mathbf{x}$ and a neighboring voxel ξ. The standard deviation σ_ζ determines up to which SSD measure the time-intensity profiles are still considered to be similar. The SSD measure is defined as

$$\zeta(\xi, \mathbf{x}) = \frac{1}{T}\sum_{t=0}^{T-1}(I(\xi(x, y, z, t)) - I(\mathbf{x}(x, y, z, t)))^2, \tag{4}$$

where T is the size of the temporal dimension, $I(\mathbf{x}(x, y, z, t))$ is the intensity value of voxel $\mathbf{x}(x, y, z)$ at time point t and $I(\xi(x, y, z, t))$ is the intensity value of a neighboring voxel $\xi(x, y, z)$ at time point t.

For each voxel $\mathbf{x}$ in the 4D dataset, the bilateral filtering equation is defined as follows:

$$\mathbf{h}(\mathbf{x}(x, y, z, t)) = \frac{1}{n(\mathbf{x})}\sum_{i=-m}^{m}\sum_{j=-n}^{n}\sum_{k=-o}^{o} I(\xi(x+i, y+j, z+k, t))c(\xi, \mathbf{x})p(\xi, \mathbf{x})\,\mathrm{d}\xi, \tag{5}$$

where m, n and o are the half kernel sizes in the x, y and z directions, respectively, $c(\xi, \mathbf{x})$ is the closeness function as defined by equation (1), $p(\xi, \mathbf{x})$ is the TIPS function as defined by equation (3) and $n(\mathbf{x})$ is the normalization factor defined as

$$n(\mathbf{x}) = \sum_{i=-m}^{m}\sum_{j=-n}^{n}\sum_{k=-o}^{o} c(\xi, \mathbf{x})p(\xi, \mathbf{x})\,\mathrm{d}\xi. \tag{6}$$

2.1. Parameter settings

As mentioned above, the parameter σ_ζ of the TIPS bilateral filter determines up to which SSD measure the time-intensity profiles are still considered to be similar. The setting of this parameter is related to the noise level in the 4D CTP scan. To determine this noise level, an area was selected in which the time-intensity profiles are assumed to be identical if no noise would be present. For cerebral CTP scans, the cerebral spinal fluid located in the ventricles was selected, by creating a mask (double threshold: 0–15 HU) on the 3D temporal average image. After erosion of the mask (cubic structure element, diameter 3 voxels), the SSD (ζ) was determined for each of the voxels within the mask (kernel size 3). The parameter σ_ζ was set to be the average SSD of all mask voxels.

The kernel size combined with σ_d determines the number of neighboring voxels included in the weighted average and the corresponding spatial weight. Increasing σ_d and therefore the kernel size will result in increased noise reduction if the time-intensity profiles of the neighboring voxels included are considered similar to the center voxel profile, based on σ_ζ. Typical values of σ_d for cerebral CTP scans range from 3 to 30 mm.

3. Experiments

The proposed TIPS bilateral filter was compared to three other noise filtering methods: the 4D bilateral filter as used by Kosior *et al* (2007), the 3D bilateral filter applied to each sequential time scan within the 4D CTP scan, and standard Gaussian smoothing in 4D. For the 3D and 4D bilateral filters, the width of the range filter (σ_r) was set to two times the standard deviation of a region of interest (ROI) placed in the white matter of the first sequential time scan as described by Kosior *et al* (2007). Since contrast enhancement is not yet present in the first sequential scan (prebolus), the standard deviation within the ROI represents noise. According to Kosior *et al* this intuitively means that neighboring intensities within a standard deviation of the prebolus white matter (i.e. noise variation) receive a high Gaussian weighting in the averaging process (Kosior *et al* 2007). For the TIPS bilateral filter, the parameter (σ_ζ) was set as described in section 2.1.

The filters were applied to the original phantom (section 3.1) and patient CTP data (section 3.2). CBF and CBV maps of the CTP scans were derived using the block-circulant singular value decomposition (bSVD) algorithm (Ostergaard *et al* 1996a, Wu *et al* 2003) available in the perfusion mismatch analyzer (PMA) software (Kudo 2010, Kudo *et al* 2010). ROIs were placed in the gray matter, white matter and infarcted area, to evaluate the mean and standard deviation of the absolute CBF and CBV values. Contrast-to-noise ratios between gray matter and white matter, gray matter and infarcted area, and white matter and infarcted area were determined as follows (Mullins *et al* 2004):

$$\mathrm{CNR} = \frac{\mu_1 - \mu_2}{\left(\sigma_1^2 + \sigma_2^2\right)^{1/2}}, \tag{7}$$

where μ is the mean CBF or CBV value of the ROI and σ is the standard deviation.

3.1. Phantom data

A CTP head phantom, with and without CT noise, was used to determine up to which extent the filtering methods could reconstruct the noise-free phantom (ground truth) by filtering the noisy phantom. The phantom consists of one slice of a human head, with realistic CT noise, anatomical structures and contrast enhancement curves. It is described in more detail below.

Since the phantom consists of one slice, the filters were applied using a 2D kernel instead of a 3D kernel in the spatial dimensions. Therefore 4D (3D + time) bilateral filtering will be referred to as 2Dt (2D + time) bilateral filtering and 3D bilateral filtering of each sequential time scan will be referred to as 2D bilateral filtering. The TIPS, 2Dt and 2D bilateral filters were applied to the noisy CTP phantom with increasing σ_d (1–29 mm). The parameters σ_r of the 2Dt and 2D bilateral filters and σ_ζ of the TIPS bilateral filter were determined as described above. Gaussian filtering was also applied with increasing spatial σ, while the temporal σ was fixed to two frames (standard setting PMA software).

CBF and CBV maps were derived from the unfiltered and filtered noisy CTP phantoms as well as from the noise-free CTP phantom. Standard smoothing of the PMA software (denoising using Gaussian filter) was used for the noisy unfiltered CTP phantom but was

turned off for the bilateral filtered and the noise-free CTP phantom. For the resulting CBF maps and the original CTP phantom data, the root mean square error (RMSE) was determined between the (un)filtered noisy CTP phantoms and the noise-free CTP phantom (ground truth). To determine the RMSE per anatomical structure, masks were used for vessels, white matter, gray matter, infarcted area and all intracranial structures.

3.1.1. Description of the CTP head phantom. Intracranial anatomical structures were segmented from a high-resolution cerebral gradient echo scan acquired on a 7 T MRI scanner (Philips Medical Systems, Best, the Netherlands). To extract the CT noise pattern, a homogeneously filled real skull was scanned using the brain perfusion protocol (150 mAs, 80 kVp, without contrast agent) on a 128-slice Brilliance iCT scanner (Philips Medical Systems, Best, the Netherlands). Multiple scans were acquired, which were averaged and subtracted from one of the CTP sequences to result in a realistic CT noise pattern. The skull (taken from the CT scan) and the segmented intracranial anatomical structures (vessels, cerebrospinal fluid and brain tissue) were combined, by non-rigidly registering the anatomical structures to fit inside the skull. All structures were assigned a base HU value corresponding to the HU value generally observed in CT scans, completing the first slice of the CTP head phantom. Since the protocol for CTP scans acquired on the 128-slice CT scanner consists of 25 sequential scans, 25 copies of this slice were used for the CTP phantom. Realistic contrast enhancement curves were added to the arteries, veins and brain tissue. The contrast enhancement curves of the arterial input function (AIF) and venous output function (VOF) were based on an average of several AIF/VOF extracted from main arteries of a CTP scan of a healthy (originally admitted with stroke symptoms) patient. The tissue contrast enhancement curves were derived by convolving the AIF with scaled residue functions created using the model described in Bredno *et al* (2010). Six brain tissue types were included: healthy, reversibly damaged, and irreversibly damaged gray and white matter. The noise-free CTP phantom was completed after simulating scanner resolution by Gaussian smoothing and partial volume effects of a 5 mm thick slice by averaging over the volume. The noisy CTP phantom used for filtering was constructed by adding the realistic CT noise to the noise-free CTP phantom.

3.2. Patient data

Scans of fifteen acute stroke patients were used for a qualitative evaluation study. These patients were consecutively selected, based on the following inclusion criteria: (1) follow-up unenhanced CT scan showed an infarction and (2) admission cerebral CTP scan showed abnormal perfusion in (and around) the area to be infarcted. Six of these CTP scans were acquired on a 64-slice and nine on a 128-slice CT scanner (Philips Healthcare, Best, the Netherlands). The sequential scans of the CTP data were acquired every 2 s during 48 s using 80 kVp and 150 mAs and 40 ml of (300 mg I ml^{-1}) contrast agent (64-slice: 5 ml s^{-1}, 128-slice: 6 ml s^{-1}). All CTP scans were reconstructed with 5 mm thick sections. The unenhanced CT scan was acquired using 120 kVp and 300 mAs. The sequential CTP time scans were registered to correct for patient motion (Mendrik *et al* 2010).

The admission patient CTP scans were filtered using the three bilateral filters (3D, 4D, TIPS). The standard deviation for the closeness measure (σ_d) was set to 9 mm for the TIPS and the 3D bilateral filter and to 5 mm (5 s in the temporal dimension) for the 4D bilateral filter, based on experiments to result in approximately the same noise reduction as the standard

settings of the Gaussian filter in the PMA software. Other parameters were set as described at the start of section 3. Of each of the filtered CTP scans, CBF and CBV maps were derived using the bSVD algorithm available in the PMA software (Kudo *et al* 2010). The Gaussian filtered maps were derived by using the standard smoothing in the PMA software, which was turned off for deriving the bilateral filtered maps.

The observer study was performed by two experienced observers (E.P.A.V. and T.v.S.). One slice, which showed the area of infarction on the CBF map, was selected in each of the 15 patient CTP scans. The follow-up unenhanced CT scans were registered to the CTP scans using a registration package (Klein *et al* 2010). The CBF maps of the filtered CTP scans were presented to the observers in pairs, together with the corresponding slice of the follow-up unenhanced CT scan (reference for infarction) and the temporal average of the original CTP scan (reference for gray/white matter differentiation). In total 120 pairs of CBF maps were blindly presented to the observers in randomized order and position (left or right). Of these 120 pairs, 90 pairs (15 patients $\times$ 6 combinations) were part of the observer study and 30 pairs (5 patients $\times$ 6 combinations) were used to check the intra-observer agreement. Observers had to either indicate which CBF map they preferred or that the maps were equal for three criteria: (1) gray/white matter differentiation, (2) detectability of infarcted area and (3) overall image quality.

4. Results

4.1. Phantom data

Figure 1 shows graphs of the RMSE between the filtered noisy CTP phantoms and the noise-free CTP phantom (ground truth) for various standard deviations (σ). The RMSE of both the original CTP data and the derived CBF maps is shown for various anatomical structures. In white matter, gray matter and the infarction, both the Gaussian filter and the 2Dt bilateral filter perform well for small standard deviations in the original CTP data. In the CBF maps, however, the performance is similar to the TIPS and 2D bilateral filters. The RMSE of the TIPS bilateral filter decreases with increasing standard deviation, while the other filters reach their minimal RMSE at smaller kernel sizes, after which the RMSE increases with increasing standard deviation. The TIPS bilateral filter shows a good correlation between the RMSE in the original CTP data and the RMSE in the CBF maps. Figure 2 shows the results of the CBF maps with the minimal RMSE for each filter. The time-intensity profiles in the top row of figure 2 show that the TIPS bilateral filter performed best in reconstructing the time-intensity profiles relative to the ground truth. Table 1 shows the mean and standard deviation of the absolute CBF and CBV values within the gray matter, white matter and infarcted area ROIs and their contrast-to-noise ratios. The mean CBF and CBV values of the TIPS bilateral filtered maps show small differences with the mean values of the ground truth with small standard deviations compared to the other filters. Furthermore, for both CBF and CBV, the contrast-to-noise ratios are highest in the TIPS bilateral filtered maps.

Figure 3 illustrates the differences in processing time between the bilateral filters. Increasing the kernel size increases the time needed for processing. Since the 2Dt filter uses a 3D kernel, it is much slower than the TIPS and 2D bilateral filters and cut off at a smaller kernel size to amplify the difference between the processing times of the TIPS and 2D bilateral filters. Figure 3 shows that the TIPS bilateral filter is faster than the 2D bilateral filter, especially for larger kernel sizes.

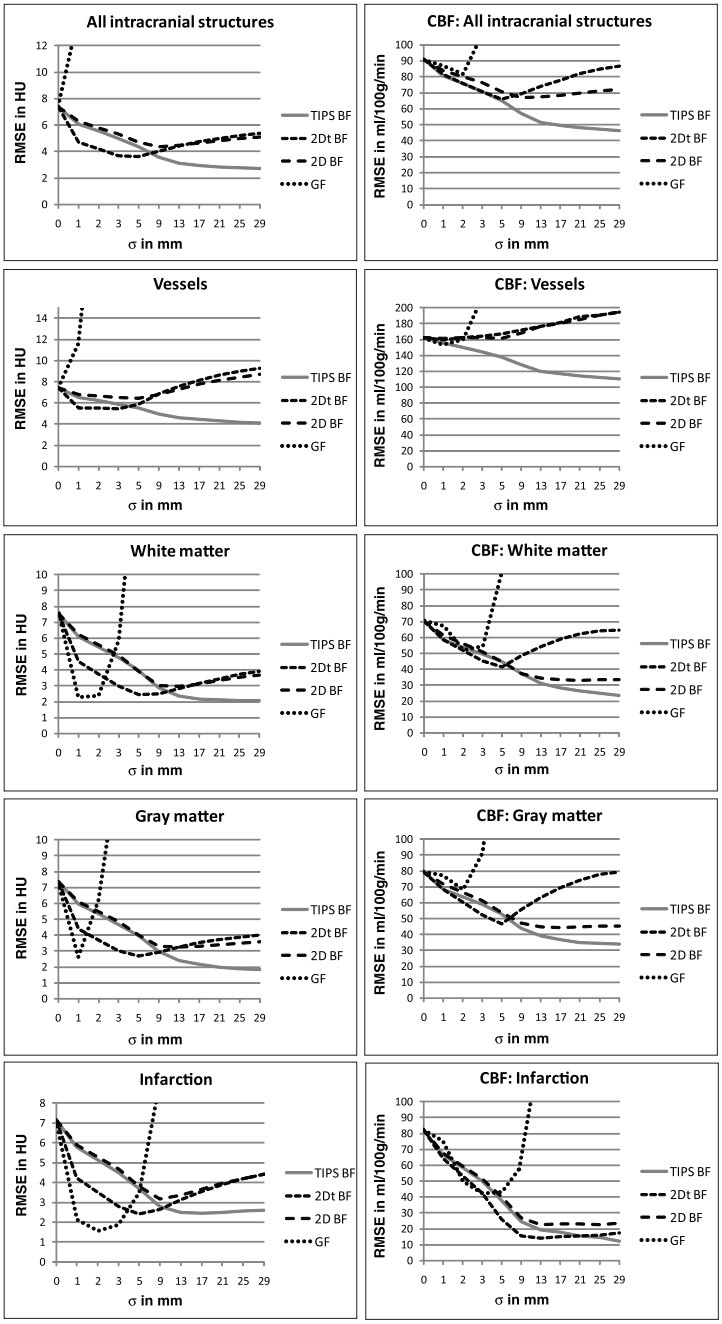

Figure 1. Graphs showing the RMSE between the filtered noisy CTP phantoms and the noise-free CTP phantom (ground truth) for increasing standard deviation (σ for the Gaussian filter (GF) and σ_d for the bilateral filters (BFs)). Increasing the spatial standard deviation increases the amount of samples taken into account in the filtering process, which could result in more noise reduction depending on the properties of the noise filter. The left column shows the results of the original CTP phantom data and the right column of the cerebral blood flow (CBF) maps derived from the CTP phantom data.

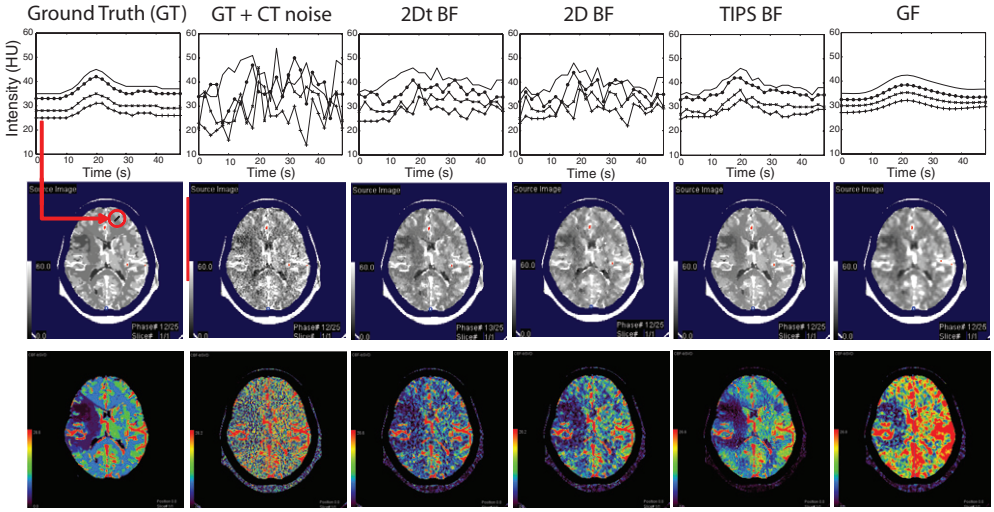

Figure 2. Results of the filtered noisy CTP head phantom. For the bilateral filters (BFs), the result with the lowest RMSE of the CBF map over all intracranial structures is shown (see figure 1 top right). The lowest RMSE for the 2Dt BF was at $\sigma_d = 5$, for the 2D BF at $\sigma_d = 9$ and for the TIPS BF at $\sigma_d = 29$. For the Gaussian filter (GF) the standard settings of the perfusion (PMA) software are used, spatial $\sigma = 4$ and temporal $\sigma = 2$. Top row: four time-intensity profiles sampled gradually from white matter to gray matter. Middle row: temporal slice 12 of the CTP head phantom. Bottom row: the CBF maps derived from the CTP head phantom using the bSVD method in the PMA software.

Table 1. Mean CBF in ml/100 g/min and CBV in ml/100 g values of ROIs in gray matter (GM), white matter (WM) and infarcted area (Inf) in the CTP phantom data. The standard deviation within the ROIs is indicated between brackets. CNR denotes the contrast-to-noise ratio; TIPS BF, the proposed time-intensity profile similarity bilateral filter and GF, the standard Gaussian filter.

CBF	White matter	Gray matter	Infarction	CNR GM–WM	CNR GM–Inf	CNR WM–Inf
Ground truth	24.2 (0.1)	39.7 (1.4)	5.30 (0.0)	10.8	24.1	165
TIPS BF	23.8 (3.5)	38.3 (3.9)	4.23 (2.7)	2.78	7.23	4.43
3D BF	25.0 (8.4)	39.3 (8.3)	10.2 (4.4)	1.22	3.10	1.57
GF	37.4 (11)	59.8 (11)	13.6 (6.8)	1.45	3.65	1.84
4D BF	21.0 (8.5)	31.3 (9.4)	11.9 (6.0)	0.81	1.74	0.88
CBV						
Ground truth	3.2 (0.0)	5.1 (0.3)	0.8 (0.0)	5.77	13.0	141
TIPS BF	3.4 (0.7)	5.3 (0.9)	0.5 (0.4)	1.60	4.83	3.43
3D BF	3.7 (1.8)	5.6 (2.0)	1.2 (1.2)	0.68	1.85	1.20
GF	5.6 (2.1)	8.5 (2.7)	1.9 (1.6)	0.87	2.13	1.40
4D BF	3.4 (2.3)	5.0 (2.5)	1.6 (1.8)	0.47	1.12	0.63

4.2. Patient data

Table 2 shows the mean and standard deviation of the absolute CBF and CBV values within the gray matter, white matter and infarcted area ROIs and their contrast-to-noise ratios averaged over all patient data. The CBF values of two of the fifteen patients were outliers and presented

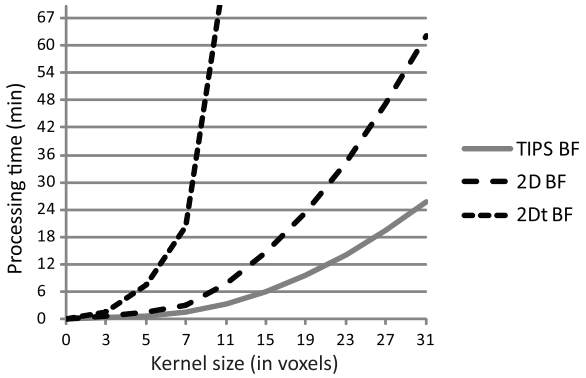

Figure 3. Graph illustrating the difference in processing time between the bilateral filters (BFs) as the kernel size is increased. For the 2D and TIPS bilateral filters a 2D kernel was used, and for the 2Dt bilateral filter a 3D kernel was used, as applied to the CTP phantom slice. Processing times were measured on a quad core 2.83 GHz PC with 8 GB of RAM. The filters were implemented in C++ and not aggressively optimized for speed.

Table 2. Mean CBF in ml/100 g/min and CBV in ml/100 g values of ROIs in gray matter (GM), white matter (WM) and infarction (Inf) averaged over all patient data. The average standard deviation within the ROIs is indicated between brackets after the mean value. CNR denotes the average contrast-to-noise ratio; TIPS BF, the proposed time-intensity profile similarity bilateral filter and GF, the standard Gaussian filter.

CBF	White matter	Gray matter	Infarction	CNR GM–WM	CNR GM–Inf	CNR WM–Inf
TIPS BF	24.2 (7.0)	50.3 (12)	11.2 (5.2)	1.93	3.10	1.56
3D BF	29.2 (10)	56.8 (17)	18.2 (8.4)	1.44	2.10	0.88
GF	34.5 (13)	72.4 (28)	22.1 (12)	1.25	1.71	0.85
4D BF	20.2 (8.2)	36.2 (13)	15.4 (7.6)	1.07	1.41	0.57
CBF[a]						
TIPS BF	0.69 (0.22)	1.61 (0.42)	0.34 (0.17)	4.62	2.04	7.60
3D BF	1.02 (0.38)	1.99 (0.62)	0.75 (0.33)	3.30	0.94	4.74
GF	1.35 (0.54)	2.95 (1.19)	1.07 (0.52)	3.63	0.58	3.90
4D BF	0.78 (0.33)	1.38 (0.53)	0.66 (0.31)	2.54	0.48	3.36
CBV						
TIPS BF	3.35 (1.1)	6.51 (1.5)	1.70 (1.2)	1.73	2.61	1.21
3D BF	3.99 (1.7)	7.49 (2.3)	2.23 (1.7)	1.28	1.89	0.85
GF	4.96 (2.5)	9.78 (4.0)	2.75 (2.4)	1.07	1.60	0.84
4D BF	3.28 (2.0)	6.31 (2.8)	2.07 (1.8)	0.96	1.40	0.59

[a]Average CBF of two outliers of which available AIF in the datasets did not lead to quantitative CBF values and were not taken into account in the overall CBF average.

separately in table 2. The reason for this was that available AIF in these datasets did not lead to quantitative CBF values. Both scans were acquired on the 64-slice scanner (4 cm coverage) near the top of the head. The contrast-to-noise ratios were however sufficient to distinguish between gray matter, white matter and infarction; therefore, the CBF maps could still be used in the observer study. In general the white matter CBF and CBV values in the

Table 3. Ranking of the noise filters (1 best, 4 worst) based on the number of times the CBF map of the corresponding filter was chosen to be best by the observer. The percentages show in how many percent of the cases (that were not chosen to be equal) the CBF map of this filter was preferred by the observer for the three criteria: (1) gray/white matter differentiation, (2) detectability of infarcted area and (3) overall image quality. TIPS BF denotes the proposed time-intensity profile similarity bilateral filter and GF, the standard Gaussian filter.

Observer 1	GM/WM differentiation	Infarction detection	Overall quality
Rank 1: TIPS BF	98%	67%	100%
Rank 2: 3D BF	38%	22%	29%
Rank 3: GF	16%	4%	7%
Rank 4: 4D BF	4%	7%	7%
Observer 2			
Rank 1: TIPS BF	89%	91%	100%
Rank 2: 3D BF	60%	47%	62%
Rank 3: GF	22%	13%	13%
Rank 4: 4D BF	7%	4%	11%

patient data were comparable to those in the phantom data. The gray matter and infarction values were higher in the patient data than in the phantom data. The TIPS bilateral filtered maps showed the best contrast-to-noise ratio and the smallest standard deviations compared to the other filters.

Table 3 shows the results of the observer study. The TIPS bilateral filter was ranked best based on the number of times the CBF maps derived from the TIPS bilateral filtered CTP scans were chosen by the observers. For the overall image quality criteria, the CBF maps of the TIPS bilateral filter were chosen in 100% of the cases by both observers. For the infarction detection criteria, the CBF maps were often scored equal. Table 4 shows in how many percent of the cases the CBF maps were chosen to be equal. Table 5 shows that when presented versus the CBF maps of the TIPS bilateral filter, none of the CBF maps of the other filters were preferred by the observers. This also holds for the gray/white matter differentiation criteria.

Kappa statistics were calculated per criterion to determine the inter- and intra-observer agreement (table 6). The majority of inconsistencies occurred when differences were subtle, in which case equal was chosen by one of the observers, while the other observer did make a decision between the two CBF maps. If we only look at the cases in which a decision in favor of a CBF map was made by both observers, the kappa statistics for inter-observer agreement increased to 0.97, 0.92 and 0.92 for gray/white matter differentiation, detection of infarcted area and overall image quality, respectively. The kappa statistics for the intra-observer agreement for observer 1 increased to 1.00 for all criteria and for observer 2 to 0.88, 0.94 and 0.93, respectively.

Figure 4 shows examples of CBF maps of four of the fifteen patient CTP scans used in the observer study. Figure 5 shows one slice of the original CTP data of one of the patients used in the evaluation, filtered with the bilateral filters, and four time-intensity profiles (two in gray matter and two in white matter).

5. Discussion

In this paper, a bilateral filtering method has been presented that uses the time–intensity profile similarity (TIPS) to reduce noise in 4D CTP scans. The TIPS bilateral filtering method was

Table 4. Scoring results showing in how many percent of the cases the observers did not prefer one CBF map above the other. In this case, the CBF maps of the filters were indicated to be of equal quality. Results are shown for the three criteria: (1) gray/white matter differentiation, (2) detectability of infarcted area and (3) overall image quality. TIPS BF denotes the proposed time-intensity profile similarity bilateral filter and GF, the standard Gaussian filter.

Observer 1	GM/WM differentiation	Infarction detection	Overall quality
TIPS BF	2%	33%	0%
3D BF	27%	60%	33%
GF	27%	53%	36%
4D BF	33%	53%	47%
Observer 2			
TIPS BF	2%	9%	0%
3D BF	18%	27%	4%
GF	11%	33%	11%
4D BF	4%	20%	11%

Table 5. Scoring results of the detectability of the infarcted area. The percentages show in how many percent of the cases the CBF map of this filter was preferred by the observer when presented versus a CBF map of one of the other filters. TIPS BF denotes the proposed time-intensity profile similarity bilateral filter and GF, the standard Gaussian filter.

Observer 1	Versus GF	Versus TIPS BF	Versus 4D BF	Versus 3D BF
GF	–	0%	13%	0%
TIPS BF	67%	–	80%	53%
4D BF	20%	0%	–	0%
3D BF	40%	0%	27%	–
Observer 2				
GF	–	0%	40%	0%
TIPS BF	93%	–	100%	80%
4D BF	13%	0%	–	0%
3D BF	53%	0%	87%	–

Table 6. Kappa statistics for determining observer agreement. The intra-observer agreement was determined on 5 of the 15 patient scans.

	GM/WM differentiation	Infarction detection	Overall quality
Inter-observer agreement	0.57	0.39	0.53
Intra-observer agreement observer 1	0.74	0.73	0.74
Intra-observer agreement observer 2	0.70	0.70	0.81

compared to Gaussian filtering, 4D and 3D (applied to each sequential scan) bilateral filtering on both phantom and real patient CTP data. CBF and CBV maps were derived from these data and evaluated.

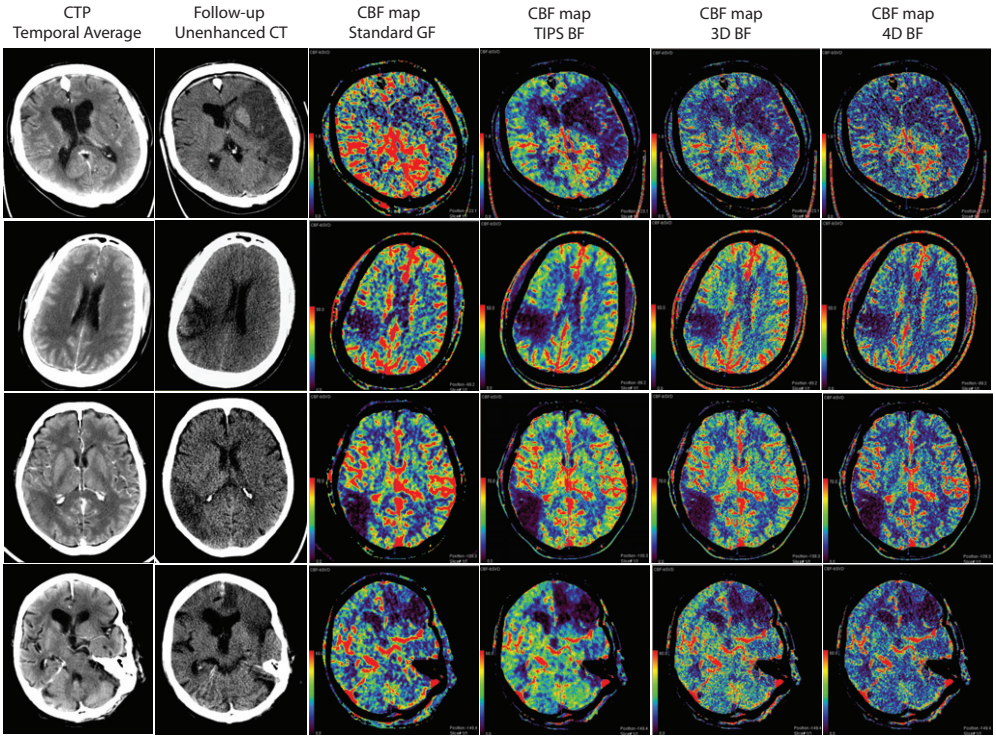

Figure 4. CBF maps of the selected slices of four of the fifteen filtered patient CTP scans used in the evaluation. In the observer study, the CBF maps were blindly presented to the observers in pairs, together with the temporal average of the original CTP scan (first column: reference for gray/white matter differentiation) and the follow-up unenhanced CT scan (second column: reference for infarction).

The CTP phantom data provided an objective test to evaluate to what extent the filters were able to reconstruct the ground truth (noise-free CTP phantom) from the noisy CTP phantom. The phantom data consisted of one slice; therefore, the bilateral filters were applied with a 2D kernel in the spatial directions. Although the patient CTP scans consist of multiple slices (3D over time), we believe that the phantom consisting of one slice (2D over time) is sufficient for the purpose of comparing the various noise reduction methods described in this paper. The patient data are routinely reconstructed with 5 mm thick slices, while the in-plane resolution is 0.39 mm $\times$ 0.39 mm. Therefore, in general, the in-plane voxels will contribute more in the weighted averaging process, based on spatial closeness, than the voxels in the slice direction. Moreover, bilateral filters are not based on structural information but on measures of spatial closeness and pixel similarity. Using a 3D kernel instead of a 2D kernel will merely result in a potential increase in the number of intensity values that are used for averaging. Therefore the phantom nicely illustrates the difference between the various properties of the bilateral noise reduction methods. Although the 2Dt (4D bilateral filtering technique on 3D data) bilateral filter performed well in terms of RMSE on the original CTP phantom data for smaller standard deviations (figure 1), it performed similar to the TIPS bilateral filter in terms of RMSE on the CBF maps. A possible explanation for this could be that although the intensity values of the original CTP phantom data approached the intensity

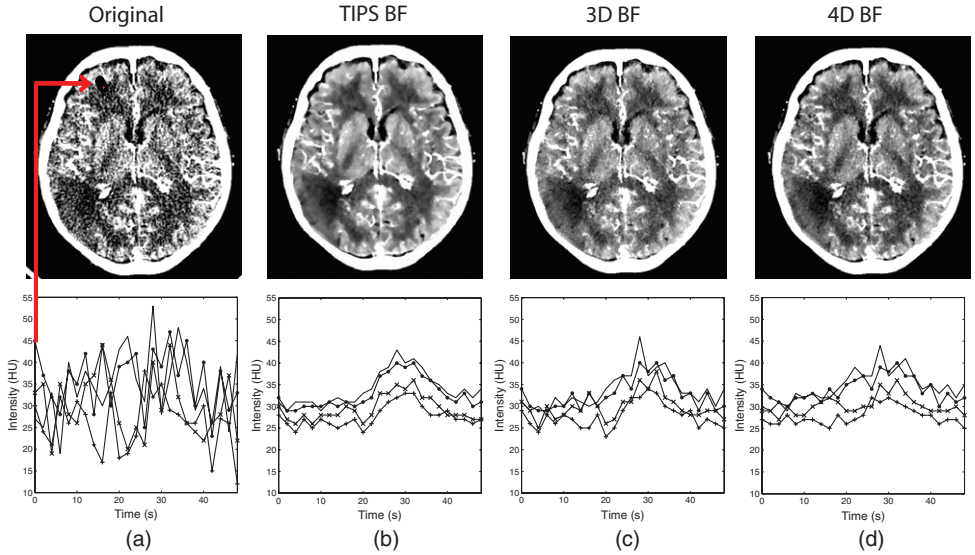

Figure 5. Example of one slice (at 28 s) of one of the 4D CTP patient scans (top row) with four time-intensity profiles (bottom row), gradually sampled from gray matter to white matter. (a) Original CTP scan. (b) Proposed TIPS bilateral filter. (c) 3D bilateral filter applied to each sequential 3D scan. (d) 4D bilateral filter.

values of the ground truth, owing to noise reduction, the shape of the time-intensity profiles (contrast enhancement curve) was not preserved. Increasing the standard deviation, enlarges the number of samples in the temporal dimension that are taken into account for averaging, which increases the influence on the time-intensity profiles and decreases the quality of the CBF maps (figure 1). The TIPS bilateral filter, however, preserves the time-intensity profiles. This is especially evident from the graph showing the RMSE of the CBF maps of the vessels and all intracranial structures in figure 1. In these graphs the TIPS bilateral filter outperforms the other filters. Within the area of infarction, all bilateral filters performed similarly. This could be due to the fact that no contrast enhancement is present within the area of infarction. Therefore intensity values in the temporal dimension are similar to the intensity values in the spatial dimensions, and thus the TIPS bilateral filter does not provide additional value in this situation.

Figure 2 shows the best results of filtering the noisy CTP phantom for all filters. From the time-intensity profiles shown in the top row, it is clear that the 2Dt bilateral filter filtered more noise from the time-intensity profiles than the 2D bilateral filter. However, the 2D bilateral filtered CBF map shows better quality than the 2Dt bilateral filtered CBF map, due to the fact that the intensity values are not averaged over time. The TIPS bilateral filtered CBF map is best able to approach the ground truth CBF map. This is also evident from the absolute CBF and CBV values presented in table 1, where the TIPS bilateral filtered values show small standard deviations and the mean values approach the values of the ground truth. The TIPS bilateral filtered maps also show the highest contrast-to-noise ratio between gray matter, white matter and infarcted area compared to the other noise reduction methods in both the phantom (table 1) and the patient data (table 2). This result is consistent with the results of the observer study on the patient CBF maps, which showed that the CBF maps of the TIPS bilateral filter

were ranked best (table 3) and chosen in 100% of the cases based on overall image quality by both observers.

CBF maps of acute stroke patients are mainly used to detect the area at risk of infarction. In most cases the CBF maps of the TIPS bilateral filter showed sharper edges and higher contrast between the area at risk of infarction and the healthy tissue (figure 4) than the CBF maps of the other filters. The CBF maps of the TIPS bilateral filter also show improved differentiation between white matter and gray matter. Gray matter is more perfused than white matter and should show a higher blood flow value in the CBF map. Therefore increased differentiation between white matter and gray matter on the CBF map signifies a higher quality CBF map. The absolute gray matter values for both CBF and CBV were higher for all the filters in the patient data than in the phantom data, while the white matter values were comparable. Since gray matter is more perfused and thus contains more vessels, a reason for this could be that in the patient data more small vessels (partial volume) were present in the gray matter ROI than in the phantom data. Although two of the fifteen patient CBF maps did not lead to quantitative CBF values, the differences between the noise reduction methods were similar to the ones presented for the quantitative CBF values. In general, the 4D bilateral filter results in an underestimation and the Gaussian filter results in an overestimation of the absolute CBF values for both white matter and gray matter. These two filters were also preferred least by the observers in the observer study on the CBF maps. The 3D bilateral filter shows similar mean CBF values as the TIPS bilateral filter, but with a much larger standard deviation. Therefore the GM–WM CNR of the TIPS bilateral filter is about 30% higher than the CNR of the 3D bilateral filter. This is consistent with the results of the observer study as well, where the CBF maps of the TIPS bilateral filter were preferred above those of the 3D bilateral filter.

6. Conclusion

An observer study on patient CT perfusion (CTP) showed that filtering 4D CTP scans with the proposed time-intensity profile similarity (TIPS) bilateral filtering method produces higher-quality cerebral blood flow (CBF) maps than applying a Gaussian, 3D bilateral or 4D bilateral filter. The TIPS bilateral filtered CBF maps were scored to have the best overall image quality in 100% of the cases by both observers. A phantom study showed that the TIPS bilateral filter preserves the time-intensity profiles in the 4D CTP scan that are essential for the calculation of cerebral blood flow, while reducing noise. Quantitative CBF and cerebral blood volume (CBV) values in both the phantom and the patient data showed that the TIPS bilateral filter resulted in realistic mean values with a smaller standard deviation than the other evaluated filters and therefore higher contrast-to-noise ratios. Furthermore, the TIPS bilateral filter is computationally faster than both the 3D and 4D bilateral filters.

Acknowledgments

This work was supported by a research grant from Philips Healthcare. The authors would like to acknowledge K Kudo for providing publicly available perfusion software (perfusion mismatch analyzer).

References

Bredno J, Olszewski M E and Wintermark M 2010 Simulation model for contrast agent dynamics in brain perfusion scans *Magn. Reson. Med.* **64** 280–90

de González A B and Darby S 2004 Risk of cancer from diagnostic x-rays: estimates for the UK and 14 other countries *Lancet* **363** 345–51

Diekmann S, Siebert E, Juran R, Roll M, Deeg W, Bauknecht H-C, Diekmann F, Klingebiel R and Bohner G 2010 Dose exposure of patients undergoing comprehensive stroke imaging by multidetector-row CT: comparison of 320-detector row and 64-detector row CT scanners *AJNR Am. J. Neuroradiol.* **31** 1003–9

Hoeffner E G, Case I, Jain R, Gujar S K, Shah G V, Deveikis J P, Carlos R C, Thompson B G, Harrigan M R and Mukherji S K 2004 Cerebral perfusion CT: technique and clinical applications *Radiology* **231** 632–44

Jain R, Hoeffner E G, Deveikis J P, Harrigan M R, Thompson B G and Mukherji S K 2004 Carotid perfusion CT with balloon occlusion and acetazolamide challenge test: feasibility *Radiology* **231** 906–13

Klein S, Staring M, Murphy K, Viergever M A and Pluim J P W 2010 elastix: a toolbox for intensity-based medical image registration *IEEE Trans. Med. Imaging* **29** 196–205

Konstas A A, Goldmakher G V, Lee T-Y and Lev M H 2009 Theoretic basis and technical implementations of CT perfusion in acute ischemic stroke: part 1. Theoretic basis *AJNR Am. J. Neuroradiol.* **30** 662–8

Kosior J C, Kosior R K and Frayne R 2007 Robust dynamic susceptibility contrast MR perfusion using 4D nonlinear noise filters *J. Magn. Reson. Imaging* **26** 1514–22

Kudo K 2010 Perfusion Mismatch Analyzer (PMA), version 3.2.0.7 http://asist.umin.jp/index-e.htm

Kudo K, Sasaki M, Yamada K, Momoshima S, Utsunomiya H, Shirato H and Ogasawara K 2010 Differences in CT perfusion maps generated by different commercial software: quantitative analysis by using identical source data of acute stroke patients *Radiology* **254** 200–9

Mayer T E, Hamann G F, Baranczyk J, Rosengarten B, Klotz E, Wiesmann M, Missler U, Schulte-Altedorneburg G and Brueckmann H J 2000 Dynamic CT perfusion imaging of acute stroke *AJNR Am. J. Neuroradiol.* **21** 1441–9

Mendrik A M, Vonken E P A, van Ginneken B, Smit E J, Waaijer A, Bertolini G, Viergever M A and Prokop M 2010 Automatic segmentation of intracranial arteries and veins in four-dimensional cerebral CT perfusion scans *Med. Phys.* **37** 2956–66

Mullins M E, Lev M H, Bove P, O'Reilly C E, Saini S, Rhea J T, Thrall J H, Hunter G J, Hamberg L M and Gonzalez R G 2004 Comparison of image quality between conventional and low-dose nonenhanced head CT. *AJNR Am. J. Neuroradiol.* **25** 533–8

Nabavi D G, LeBlanc L M, Baxter B, Lee D H, Fox A J, Lownie S P, Ferguson G G, Craen R A, Gelb A W and Lee T Y 2001 Monitoring cerebral perfusion after subarachnoid hemorrhage using CT *Neuroradiology* **43** 7–16

Ostergaard L, Sorensen A G, Kwong K K, Weisskoff R M, Gyldensted C and Rosen B R 1996a High resolution measurement of cerebral blood flow using intravascular tracer bolus passages: part II. Experimental comparison and preliminary results *Magn. Reson. Med.* **36** 726–36

Ostergaard L, Weisskoff R M, Chesler D A, Gyldensted C and Rosen B R 1996b High resolution measurement of cerebral blood flow using intravascular tracer bolus passages: part I. Mathematical approach and statistical analysis *Magn. Reson. Med.* **36** 715–25

Prasad K N, Cole W C and Haase G M 2004 Radiation protection in humans: extending the concept of as low as reasonably achievable (ALARA) from dose to biological damage *Br. J. Radiol.* **77** 97–9

Tomasi C and Manduchi R 1998 Bilateral filtering for gray and color images *Proc. 6th Int. Conf. on Computer Vision* pp 839–46

Wintermark M 2005 Brain perfusion-CT in acute stroke patients *Eur. Radiol.* **15** (Suppl. 4) D28–31

Wintermark M, Rowley H A and Lev M H 2009 Acute stroke triage to intravenous thrombolysis and other therapies with advanced CT or MR imaging: pro CT *Radiology* **251** 619–26

Wittsack H J, Wohlschläger A M, Ritzl E K, Kleiser R, Cohnen M, Seitz R J and Mödder U 2008 Ct-perfusion imaging of the human brain: advanced deconvolution analysis using circulant singular value decomposition *Comput. Med. Imaging Graph.* **32** 67–77

Wu O, Ostergaard L, Weisskoff R M, Benner T, Rosen B R and Sorensen A G 2003 Tracer arrival timing-insensitive technique for estimating flow in MR perfusion-weighted imaging using singular value decomposition with a block-circulant deconvolution matrix *Magn. Reson. Med.* **50** 164–74